JOURNAL OF SPACECRAFT AND ROCKETS
Vol. 44, No. 6, November–December 2007

Atmospheric Density During the Aerobraking of Mars Odyssey from Radio Tracking Data

Erwan Mazarico* and Maria T. Zuber†
Massachusetts Institute of Technology, Cambridge, Massachusetts 02139
and
Frank G. Lemoine‡ and David E. Smith‡
NASA Goddard Space Flight Center, Greenbelt, Maryland 20771

DOI: 10.2514/1.28448

We analyzed X-band radio tracking observations of the Mars Odyssey spacecraft during its aerobraking phase (October 2001–January 2002). Using the precision orbit determination software GEODYN, we obtained estimates of the spacecraft orbital energy lost during each periapsis pass due to atmospheric drag. We also recovered atmospheric density values at each periapsis, assuming simple exponential atmospheric models. Our measurements are in good agreement with the time series from the Odyssey accelerometer instrument, but they are dependent on the a priori scale height used. Using the accelerometer-derived periapsis densities and the precision orbit determination-derived frictional loss of orbital energy, we calculated new scale heights. Each represents the effective scale height of the atmosphere near periapsis for each aerobraking pass. Our results are consistently $\approx 1.7 \pm 0.7$ km greater than the published accelerometer values. The accelerometer measurements have higher spatial and temporal resolution when they are available, but these results provide a data set useful for engineering and navigational purposes, to assess variability in the Martian middle atmosphere.

Nomenclature

A	=	spacecraft cross section
a	=	semimajor axis
C_D	=	drag coefficient
C_R	=	radiation coefficient
E_i	=	orbital energy of aerobraking orbit i
e	=	orbital eccentricity
G	=	gravitational constant
H	=	atmospheric scale height
M	=	mass of Mars
r	=	distance to Mars center of mass
r_0	=	reference distance to Mars center of mass
z	=	altitude above reference ellipsoid
z_0	=	reference altitude above reference ellipsoid
θ	=	orbital true anomaly
ρ	=	atmospheric density
ρ_0	=	atmospheric density at the reference altitude z_0
σ_{ACC}	=	sigma for the atmospheric scale height published by the Accelerometer Team
σ_{POD}	=	uncertainty on the atmospheric scale height obtained from this study

I. Introduction

IN ADDITION to the obvious scientific interest in understanding the density structure and variability of the middle atmosphere of Mars, there are strong engineering incentives to do so. Such knowledge is critical to lander entry, and to orbiter aerobraking operations. Given the numerous planned missions to Mars, and with the perspective of human exploration, significant effort has been invested into collecting data on Mars' atmospheric structure. Thus, the amount of data available for modeling and understanding the lower and middle atmosphere has increased considerably. In addition to radio occultation and remote sensing studies during the primary missions of the various spacecraft in orbit around Mars, accelerometer experiments have been conducted during aerobraking. Accelerometers on Mars Global Surveyor (MGS), Mars Odyssey and Mars Reconnaissance Orbiter (MRO) obtained density profiles at each passage through the denser layers of the atmosphere, from periapsis up to about 140 km altitude [1–4].

Here we present density measurements of the middle atmosphere of Mars using the radio tracking data of the Mars Odyssey spacecraft during its aerobraking phase (24 October 2001 to 11 January 2002). Mars Odyssey, launched on 7 April 2001, performed its Mars orbit insertion maneuver on 24 October 2001, achieving an initial 18.6-h-long and highly elliptical orbit. Slowly, thanks to the atmospheric drag, the semimajor axis and the eccentricity of the orbit were decreased to reach the final, nearly circular mapping orbit.

In this study we show that Precise Orbit Determination (POD) can be used during periods of high atmospheric drag to estimate the energy lost by friction and the atmospheric environment near periapsis. POD has been used in the past to conduct studies geared toward the Martian atmosphere [5–9], but previous studies used data at higher altitudes (MGS near 175 and 400 km; Mars Odyssey near 400 km).

The Mars Odyssey spacecraft also included an accelerometer that was used during the aerobraking phase to estimate atmospheric density to aid in spacecraft operations. A preliminary reexamination of the raw accelerometer data[§] showed some differences in the recovered density values compared with initial values published by the Accelerometer Team [10]. Because POD uses an independent data set, it can provide a complementary view of the atmospheric density environment. Here we present periapsis density and scale height results, assuming an exponential atmosphere with constant scale height. These results are used to assess atmospheric variability,

Presented as Paper 6391 at the AIAA/AAS Astrodynamics Specialist Conference, Keystone, CO, 21–24 August 2006; received 20 October 2006; revision received 26 February 2007; accepted for publication 10 May 2007.

*Graduate Student, Department of Earth, Atmospheric and Planetary Sciences. Student Member AIAA.
†E. A. Griswold Professor of Geophysics, Department of Earth, Atmospheric and Planetary Sciences.
‡Geophysicist, Solar System Exploration Division.

§See Withers, P. G., "Rapid Data Products from the ODY ACC Experiment Generated in Support of MRO Aerobraking," http://sirius.bu.edu/withers/odyaccresultformro_v1point0/ [retrieved 26 July 2006].

which could be useful to make predictions when no accelerometer data are available.

II. Data and Methods

Compared with previous analyses performed during mission science phases [7,8,11], where the atmospheric drag acceleration is very small compared with radiation pressure accelerations (both direct and reflected by Mars), the drag acceleration levels during Mars Odyssey aerobraking are 4 to 5 orders of magnitude larger. This is, of course, due to the much lower altitude during this mission phase: the periapsis altitude is in general around 100–110 km, compared with a mean mapping phase altitude of around 390–400 km. During each passage through periapsis, the friction decreases the total energy of the spacecraft orbit. The change in energy corresponds to a change in orbital parameters (ideally, only the semimajor axis), shrinking the orbit (the very objective of aerobraking).

The Mars Odyssey orbit and the atmospheric density are thus closely related. Although the accelerometer measurements do not invoke the particular geometry of the orbit (except through the spacecraft velocity, to transform the observed acceleration into a density), it is possible to estimate the atmospheric density at periapsis from the trajectory alone.

A. Simple Timing Method

To illustrate that point, and to assess whether we could anticipate valuable results with a more precise approach, we conducted preliminary calculations of the periapsis density using two relatively straightforward methods. We first used theoretical results [12], which give a direct relationship between the eccentricity, the change in semimajor axis and the density at the periapsis. Our second method was more computational. For each aerobraking pass, we extracted positions of the Mars Odyssey spacecraft from the SPICE [13] kernels on the NASA Planetary Data System (PDS). The orbital energy change was calculated from the semimajor axis values at the preceding and following apoapsis:

$$\Delta E_i = E_{i+1} - E_i = -\frac{GM}{2}\left(\frac{1}{a_{i+1}} - \frac{1}{a_i}\right) \tag{1}$$

During aerobraking, the loss of energy by atmospheric drag is much larger than changes in semimajor axis due to secular effects or orbit perturbations, and so we have $\Delta E_i < 0$. A simple atmospheric exponential density model

$$\rho(z) = \rho_0 \exp\left(-\frac{z - z_0}{H_0}\right) \tag{2}$$

was used to obtain the energy lost by friction along the trajectory arc. Each discretized 1 s orbital segment contributed

$$\tfrac{1}{2} C_D A \rho(z) V(z)^2 \cdot \mathrm{d}s \tag{3}$$

to the total dissipated energy E_{diss} (where ds is the length of the segment, A is the cross-sectional area of the spacecraft, C_D is the drag coefficient, and V is velocity). The atmospheric density ρ_0 at the reference height z_0 was adjusted so that $\Delta E = E_{\mathrm{diss}}$. The density at periapsis was then obtained.

As seen in Fig. 1a, the densities obtained from both methods (with $H_0 = 10$ km) are in general agreement with results from the accelerometer experiment, in terms of magnitude and trend. The densities are consistently underestimated by ~20% (Fig. 1b), and larger discrepancies appear when the semimajor axis decreases (aerobraking pass number >250). Nevertheless it is sensible to expect more accurate estimates of the density during the Mars Odyssey aerobraking phase using POD than provided by oversimplified methods.

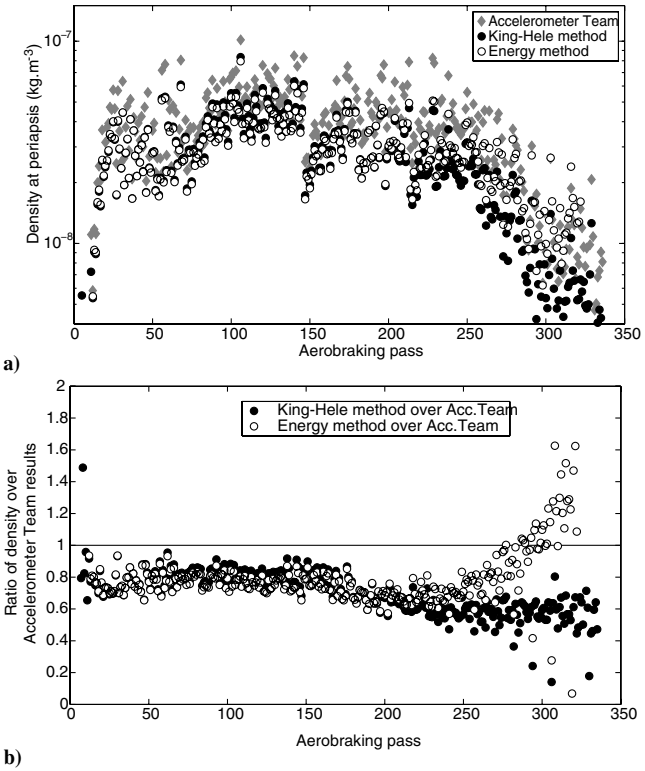

Fig. 1 a) Time series of the preliminary periapsis densities compared with accelerometer-derived results. b) Density ratios show that while there is general agreement, large discrepancies appear when the orbit semimajor axis decreases.

B. Precise Orbit Determination

1. Methods and Models

Compared with the previous methods, precise orbit determination (POD) has the advantage of providing a rigorous framework with which to evaluate the contribution of atmospheric drag to orbit evolution, relative to those caused by other forces acting on the spacecraft. Physical models of the geometry, the forces, and the corrections to be applied to the tracking observations are used to integrate the trajectory of the spacecraft (called an "arc"). The initial state of the spacecraft and various parameters describing those physical models are adjusted according to the differences (residuals) between actual observations and best-fit values inferred from the reconstructed trajectory. This process is iterated until an accurate fit is found, which minimizes the residuals of the observations. In this manner, POD can help disentangle atmospheric drag from contributions from other forces. We used the GEODYN program, developed at NASA Goddard Space Flight Center (GSFC) [14]. GEODYN is an orbit determination least squares batch filter that integrates the equations of motion and processes spacecraft tracking data to estimate geodetic parameters. On the force model side, gravitational accelerations of the sun, Earth, moon, planets, Phobos and Deimos are calculated based on the DE410 planetary ephemerides [15,16]; for Mars itself, a degree and order 90 spherical harmonic model (the GSFC "mgm1041c") is used[¶]; modeled nonconservative accelerations include direct solar radiation, albedo and thermal planetary radiation, and atmospheric drag. GEODYN also applies corrections to the tracking data for relativity, for spacecraft antenna offset, for tropospheric delay due to ground station weather, and for ground station position due to polar motion, solid tides, and ocean loading. The values used for these parameters

[¶]See Lemoine, F. G., "MGM1041c Gravity Model, Mars Global Surveyor Radio Science Archival Volume MGS-M-RSS-5-SDP-V1/mors_1021," http://pds-geosciences.wustl.edu/geodata/mgs-m-rss-5-sdp-v1/mors_1021/sha/ [retrieved 22 February 2007].

are the same as in studies of Mars Global Surveyor and Mars Odyssey mapping phase radio tracking data [8,17].

Compared with previous studies, we changed the a priori atmospheric model. Instead of using the Stewart model [18], based on the dual snapshot Viking lander entry profiles, we used a simple exponential model, which is better adapted to the middle atmosphere. The scale height is set, but the a priori density of 2×10^{-8} kg $\cdot$ m^{-3} at a reference height of 110 km is adjusted by GEODYN, through the drag coefficient C_D.

2. Data

Although there is no official radio science investigation on Mars Odyssey, the raw radio tracking data and the timings of the orbital maneuvers have fortunately been archived on the NASA PDS server by R. A. Simpson. We analyzed data between 2 November 2001 and 9 January 2002, that is, about 300 aerobraking passes (#12 to #313, referenced to #2 at ~21:05UTC on 24 October 2001). No radio tracking data were available between 31 December 2001 and 8 January 2002, corresponding to aerobraking passes #187 to #272.

The two types of observables in the tracking of the Mars Odyssey spacecraft are Doppler and Range measurements. In simple terms, Doppler observations constrain the velocity of the spacecraft relative to the tracking ground station, but only in the line-of-sight to the observing station on Earth. Range observations, usually more sparse, measure the ground station to spacecraft distance. In the case of Mars Global Surveyor and Mars Odyssey (science phase), the uncertainty in those measurements is usually ~0.1 mm/s and 1 m, respectively. However, the aerobraking radio tracking data available are based on 1-s averages, instead of typical 10-s averages. Thus, the expected standard deviations on the Doppler measurements would be closer to ~0.3 mm/s (increase by a factor $\sqrt{10}$). On the other hand, as a consequence, the number of observations is comparatively much greater. During the ~2 months (68 days) of data processed in this study, there were ~4,000,000 Doppler and ~30,000 range observations to compare to ~3,500,000 and ~155,000, respectively, during ~4 yr of the Mars Odyssey mission [8]. This large number is also due to a necessarily more comprehensive tracking during aerobraking, which is the most critical phase of the mission once in orbit around Mars.

The observation geometry of the orbit during the aerobraking phase, as well as practical constraints on the spacecraft attitude during atmospheric passes, lead to poor periapsis tracking coverage (the high-gain antenna, HGA, was stowed on the spacecraft bus during drag passes). Only four passes were tracked during periapsis. In general, there was a data gap, extending around periapsis by ± 20 min (minimum: 12 min, maximum: 30 min). To verify that the estimated C_D on the great majority of the arcs was not biased due to those data gaps, we artificially removed 40 min of data around the four periapsis with actual data. The drag coefficient adjusted by GEODYN changes by less than 0.1% in three cases, and by ~0.5% at maximum. Thus, this lack of coverage just near periapsis does not bias our results. On the other hand, without coverage near periapsis, we cannot constrain atmospheric model other than simple exponential density models. Note that to be able to put any constraint on the atmospheric density, it is necessary to constrain the orbit both before and after the atmospheric drag pass occurs. Thus, any aerobraking pass that lacked tracking on either side (ingress or egress) was discarded.

3. Arcs

Performing the orbit determination on arcs several orbits in length proved difficult because of frequent orbital maneuvers. During aerobraking, those maneuvers are generally short but quite numerous, and take place mostly near periapsis, and usually with no data coverage. Instead of letting GEODYN adjust every single thruster firing documented on the PDS, we grouped them in longer "maneuvers." Distinguishing and estimating numerous second-long thruster firings could lead to a destabilization of the solution, and so instead we estimated one single set of accelerations per periapsis maneuver. There are two short periods free of maneuvers, and longer arcs, each spanning ~10 orbits, yield reasonable estimates of density. In total, we created 179 separate arcs.

The processing of the arc is not as straightforward as during the mission mapping phase. The main difficulty comes from the initial state value. This initial "guess" to start the integration is based on the available SPICE kernels (reconstruction from the Navigation Team). Starting the arc near apoapsis made the POD program (GEODYN) overcorrect the initial state after the first iteration and often lead to nonconvergence. For this reason, we chose to start the arcs as close to Mars as possible, so that the uncertainties in the initial position, and hence in the adjustments, are necessarily smaller. To use as much tracking data as possible, the arcs were generally started shortly after the previous periapsis (once the altitude of the spacecraft was above the atmosphere contributing to the pass drag, taken to be ~300 km). Similarly they were stopped before entering the atmosphere at the following aerobraking pass. Each arc thus lasted for a bit less than two orbital periods.

In addition, we generally performed initial convergence of the arcs assuming a fixed initial state. This enabled the removal of "bad" data points, another source of solution instability. The constraints on the initial state were then loosened, and we obtained the adjusted values for the parameters of interest (below).

III. Results

A. Arc Convergence

The quality of the arc convergence can be assessed from the residuals. We obtain root mean squares (rms) values of arc residuals of order of 5–10 mm/s. This is greater than common values for the higher-altitude science phase arcs of MGS and Mars Odyssey [8,11] (where the rms is less than 1 mm/s). Indeed with more elliptical and higher-energy orbits, small changes in the adjusted orbital elements lead to more significant changes in position and velocity along the arc. Nevertheless the arc convergence is stable, and estimates of the drag coefficient, the critical physical parameter for our purpose, are robust.

The magnitude of the solar radiation pressure forces (direct solar radiation and reflected solar radiation due to Mars albedo) are scaled by a radiation coefficient C_R, which is also adjusted by GEODYN during the POD processing. The recovered coefficients are quite different from unity, as would be expected ideally. The "contamination" of C_R entails insufficient force modeling; either the radiation pressure itself or other forces are wrongly accounted for by GEODYN. The Mars Odyssey spacecraft has only one solar panel, and the asymmetry in its geometry could enhance residual forces not properly modeled.

Our modeling of the radiation pressure is arguably not thorough. Indeed the spacecraft attitude is not considered because of important self-shadowing due to the stowed HGA and frequent quaternion telemetry gaps not straightforward to interpolate. For those reasons, we fixed the cross section to a value of 11 m^2. This is a fair assumption near periapsis because the spacecraft was controlled such that it presented the $-Y$ face to the air flow. Outside of the atmosphere (which accounts for the major part of the orbit), the attitude of the spacecraft is not constrained as well, and using a constant cross-sectional area for the radiation force along the whole orbit might result in significant errors in its modeling. However, during aerobraking, over an entire orbit, the atmospheric drag is much stronger than the radiation pressure. (The opposite is true during normal science phase.) In addition, radiation effects over a couple of orbits are not as important as in the case of long arcs at higher altitude.

The adjusted C_R values are generally low, meaning that the mismodeled forces that are contaminating the C_R recovery are small compared with the atmospheric drag. The inexact recovery of C_R is thus not a subject of worry for the quality of the adjusted C_D values. To demonstrate this, we processed all the arcs both with C_R fixed to 1 and with C_R unconstrained. The ratio of the two obtained C_D series has a mean of exactly 1.0, and a standard deviation of only 0.5%.

The recovery of the magnitude of the orbital maneuvers is of the same order as the values reconstructed from the PDS. Given the

important differences between modeled (one rather long and continuous acceleration) and actual (numerous short thruster firings) maneuvers, we did not expect perfect agreement. In any case, the magnitude of these maneuvers is generally rather small compared with the atmospheric drag acceleration, and so the impact on the adjusted C_D should also be small. We verified this by reprocessing the aerobraking tracking data constraining the accelerations to the PDS values, not allowing GEODYN to adjust them. The recovered C_D values are very close to our previous results. The mean of the C_D values changes by only 0.5%, with a 1.5% standard deviation.

B. Density Estimates

We obtain the density measurements at the periapsis from the C_D time series. The measured density at the reference height of 110 km is simply the drag coefficient multiplied by our a priori 2×10^{-8} kg · m^{-3}. Using the scale height of the simple exponential model used during POD, we calculate the density at the periapsis altitude, where most of the atmospheric drag occurs, that is to say where the measurement is actually done, and meaningful.

IV. Discussion

A. Density Comparison

For comparison with published density results during aerobraking, we refer only to densities at periapsis, because that is where the drag force acts on the spacecraft and thus where our measurements are significant. Furthermore, differences in scale heights between models would artificially increase the discrepancies between our measured values and the accelerometer-derived densities when referencing them to a common reference altitude. The periapsis is also a natural choice for comparison because the Accelerometer Team did not detail its definition of the reference ellipsoid for the altitude reference. A disadvantage of dealing with periapsis densities is that the plots presented here cannot be directly used to infer any temporal variation, because the periapsis altitude varies over time.

Figure 2a shows the densities at periapsis obtained from POD, the published values from the Accelerometer Team and the values obtained by Withers on preliminary reexamination of the same accelerometer data. The POD approach shows a clearly improved agreement with accelerometer-derived results compared with the simple methods presented in Sec. II.B. Recovered densities are in closer agreement with the Accelerometer Team results than the more recent calculations by Withers (derived from either 1s-, 7s- or 39s-smoothed raw accelerometer data). Varying the smoothing applied does bring changes to the recovered density profiles. In particular, the 39-s densities can be 10% lower than the and 7-s samples. Therefore, we prefer using the 7-s estimates, which have the advantage of both giving periapsis densities very close to the 1-s values and showing the overall density structure (and not the waves or instabilities).

B. Scale Height Comparison

In Fig. 2b, we plot the ratio of various densities with the Accelerometer Team results. The time series corresponding to the POD with a scale height of 10 km actually shows less scatter around unity than densities obtained from the 7s-smoothed data (itself closer to the previously published accelerometer results than the 1 and 39-s cases).

The density recovery is stable for shorter orbital periods, unlike the divergence observed earlier (Sec. II.B). The scatter around accelerometer-derived results is greatly reduced. When the model scale height is decreased (from 10 to 5 km), the obtained densities increase, because the same amount of friction must be experienced along a much shorter arc length (most of the drag occurs within two or three scale heights above the periapsis). Likewise increasing the scale height (from 10 to 15 km) leads to smaller estimates of the density near periapsis. For an a priori scale height of 10 km, the density ratios, very close to 1 before the radio tracking data gap (orbit number <186), are ≈0.8 afterwards. The scale height decreased from ≈10 km to ≈6 km. The evolution of important parameters is shown on Fig. 3. Several of them do show correlation or

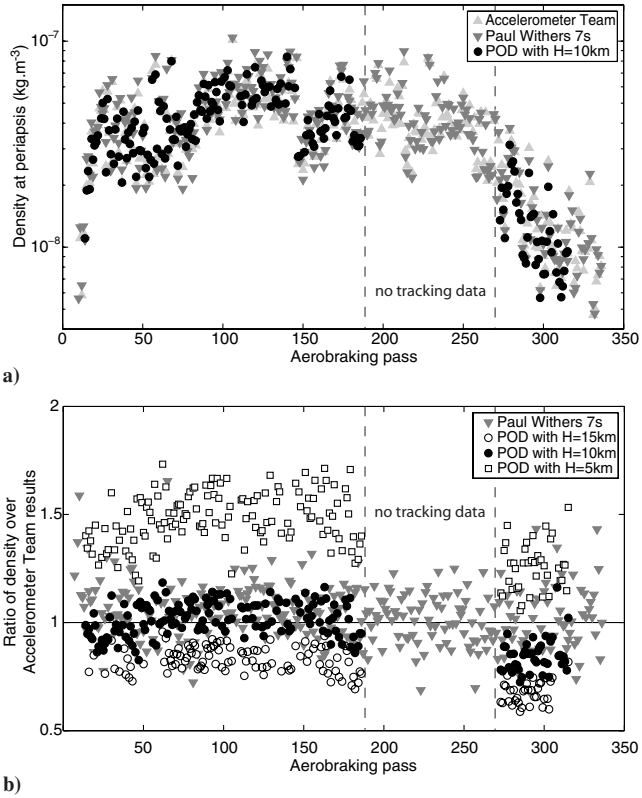

Fig. 2 a) Time series of the periapsis densities determined by POD compared with accelerometer-derived results by the Accelerometer Team and P. Withers. b) The retrieved periapsis density depends on the a priori scale height chosen during the tracking data analysis. In the ratios shown here, a value of 10 km leads to the best agreement with the densities published by the Accelerometer Team, with a scatter around unity comparable to that of the reanalysis of the raw accelerometer data by P. Withers.

anticorrelation with the scale height obtained from the accelerometer experiment: latitude, local solar time, altitude. The changes in solar-zenith angle are rather small compared with those. With the POD method used here, the assumed scale height plays an important role on the measured density. Figure 4 shows the density ratios obtained

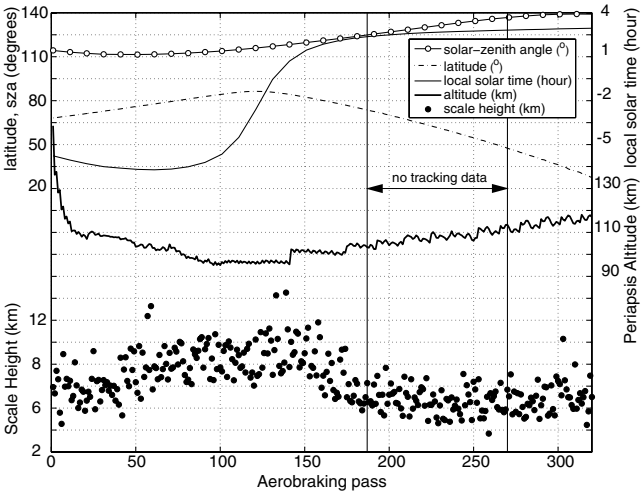

Fig. 3 Scale height obtained from the Accelerometer Experiment (solid circles) versus orbit number. Also plotted are the parameters that influence the atmospheric scale height: solar-zenith angle, latitude, local solar time and altitude. The values are given at periapsis. The region of the atmosphere sampled changes significantly during the tracking data gap, going in latitudes from ≈70–80° N to ≈30–50° N.

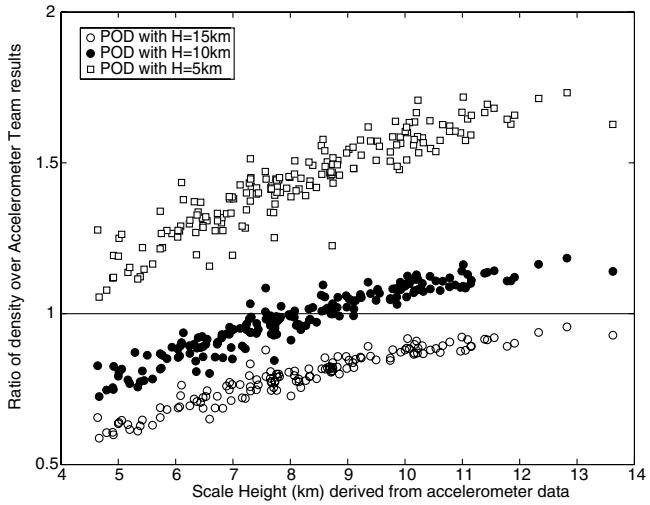

Fig. 4 When plotted against Accelerometer scale height, the discrepancy between Accelerometer densities and our results plots nearly linearly. The ratio is close to 1 when $H_{ACC} \sim H_{POD}$.

from POD plotted against the scale height derived from the accelerometer experiment. From a nearly random scatter around unity in Fig. 2b, a clear linear trend appears, supporting the fact that the obtained ratio is closer to unity when the assumed scale height is closer to the actual scale height. GEODYN does not currently have the capability to dynamically adjust the scale height during the arc convergence. The variations shown on Fig. 3 clearly show that assuming a constant scale height is not correct. However, the choice of reasonable time-variable values would suppose a good a priori knowledge of the atmosphere

In reality, POD analysis of the tracking data produces precise estimates of ΔE, the energy lost by friction over one orbit. This quantity does not depend on the a priori atmospheric models used, and converging the same arcs with various scale heights leads to reasonably close values. The relative uncertainty in ΔE is <5%, rising with time from $1 \pm 1\%$ to $2 \pm 2\%$ (Fig. 7). For the most part, this increase is due to the decreasing orbit semimajor axis, and the decrease of the ratio lost frictional energy over total orbit energy.

On the other hand, as said above, the density is better constrained by the accelerometer, because of the high signal-to-noise ratio near periapsis. Thus, a new estimate of the scale height consistent with both the accelerometer periapsis density and the total frictional energy lost in an orbit can be obtained by solving for

$$H_{NEW} \quad \text{such that } \Delta E(\rho_{ACC}, H_{NEW}) = \Delta E(\rho_{POD}, H_{POD}) \tag{4}$$

We use the periapsis density determined from the accelerometer data. We choose to use the Accelerometer Team results, for consistency reasons in the following comparison of our estimated scale heights with the Accelerometer Team scale heights; and because the results obtained by Withers did not take the dependence of C_D on density (transitional regime) into account. We were cautious of wave activity near periapsis for the evaluation of periapsis density.

To relate the frictional energy to orbital parameters and density and scale height at periapsis, we use simple orbital mechanics. On an orbit with semimajor axis a and eccentricity e, the distance to the center of the planet r is given by

$$r(\theta) = \frac{a(1-e^2)}{1 + e\cos(\theta)} \tag{5}$$

where θ is the true anomaly ($\theta = 0$ at periapsis). Over a short arc length $ds = r \cdot d\theta$ at position θ, the energy lost due to friction is

$$dE(\theta) = \left(\frac{1}{2} C_D \rho(\theta) V(\theta)^2 A\right) \cdot ds = \frac{C_D A}{2}\left[\rho_0 \exp\left(-\frac{r(\theta) - r_0}{H_0}\right)\right] \cdot \left[GM\left(\frac{2}{r(\theta)} - \frac{1}{a}\right)\right] \cdot r(\theta)\, d\theta \tag{6}$$

Integrating over θ from $-\pi$ to π (to obtain the total energy loss over one orbit), we obtain:

$$\Delta E = \frac{C_D A G M}{2} \rho_0 f(a, e, r_0, H_0) \tag{7}$$

with

$$f(a, e, r_0, H_0) = \int_{-\pi}^{\pi} \frac{1 + 2e\cos(\theta) + e^2}{1 + e\cos(\theta)} \exp\left(-\frac{\frac{a(1-e^2)}{1+e\cos(\theta)} - r_0}{H_0}\right) d\theta \tag{8}$$

Thus, the new estimate of the scale height has to satisfy:

$$H_{NEW} \quad \text{such that } f(a, e, r_0, H_{NEW}) = \frac{\rho_{POD}}{\rho_{ACC}} f(a, e, r_0, H_{POD}) \tag{9}$$

For each aerobraking arc, we performed a least-square inversion to obtain the scale height that best fits the results obtained with all the probed a priori scale heights. The uncertainty was estimated from the scatter of scale heights inferred from individual a priori scale heights around that best-fit value (see Fig. 5 for explanation). The comparison between the POD and the accelerometer results is shown in Fig. 6.

We processed the entire aerobraking data set using 12 model scale heights (from 4 to 15 km, every kilometer), so that the uncertainties (σ_{POD}) are small: 350 ± 150 m, with a maximum of 900 m. These uncertainties are mostly due to uncertainties in ΔE, and thus follow the same trend, increasing with time from $1.5 \pm 1\%$ to $4 \pm 3\%$ (Fig. 7). They cannot be compared with the uncertainties published by the Accelerometer Team (σ_{ACC}), which measure the departure of the actual density profile from an exponential one. With POD it is not

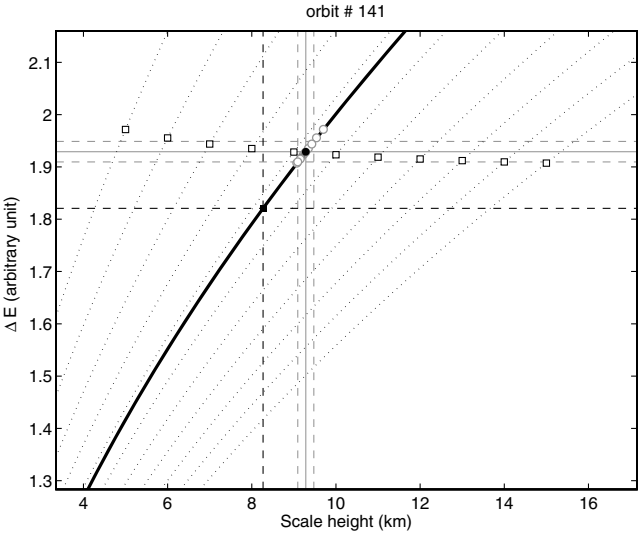

Fig. 5 Technique used to obtain new estimates of the atmospheric scale height. This example is based on orbit #141. The various curves relate the frictional energy to the scale height, given a particular density at periapsis. The thick solid line shows such a curve with the density at periapsis measured by the accelerometer. The solid square is placed at the accelerometer-derived scale height, and gives the ΔE lost by friction that can be inferred from the accelerometer results. The dotted lines and open squares are the same, for the various GEODYN runs. Each GEODYN-measured ΔE is used to infer a new scale height (open circles) consistent with the accelerometer periapsis density. These new values are used to calculate a least-square best-fit (solid circle) and associated sigma (vertical dashed light-gray lines).

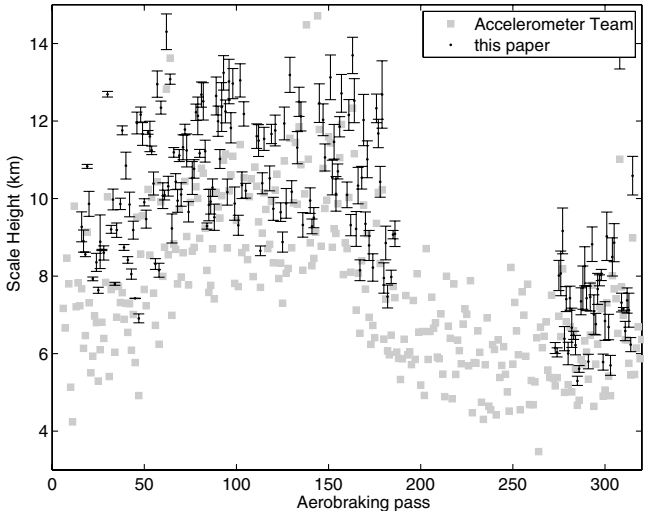

Fig. 6 Scale heights obtained from POD, with their 1-sigma uncertainties, and scale height values inferred from the accelerometer experiment (light gray squares; uncertainties are not shown but are $\approx 1.9 \pm 1.6$ km).

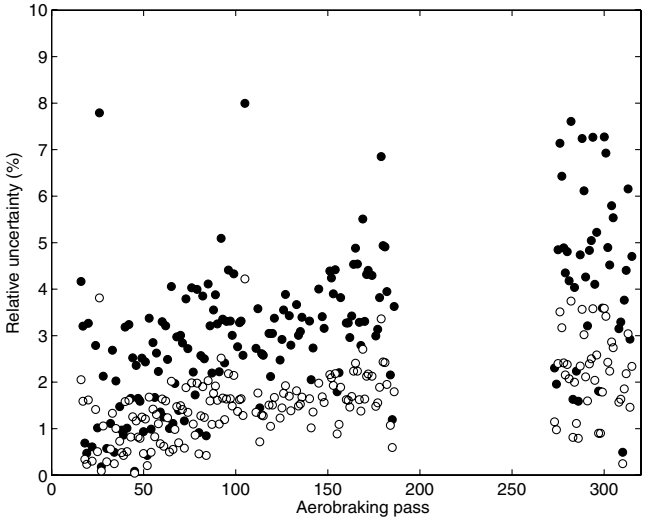

Fig. 7 Relative uncertainties (in percent) of the recovered scale height (H, solid circles) and of the frictional energy lost during the aerobraking pass (ΔE, open circles).

possible to obtain density measurements at high spatial and temporal resolution because of the scarcity of radio tracking data relative to the number of parameters that would need to be estimated. Thus, our uncertainties represent the level of confidence in the exponential profile scale height.

From Fig. 6, it is clear that for the most part the obtained scale heights are larger than the published Accelerometer Team values. When plotted against each other (Fig. 8), we observe an almost constant bias offset between the two series: our recovered scale heights are $\approx 1.7 \pm 0.7$ km larger. This suggests that ΔE would be consistently underestimated from the accelerometer data alone, by about $\approx 9 \pm 3.5\%$. Furthermore, about 86% of the Accelerometer Team scale heights do not fall within 3-sigma of our determined values.

It is important to note that when the assumption of an exponential atmosphere is verified (low σ_{ACC}), the scale heights obtained from both methods are in good agreement. All of the periapsis passes with $\sigma_{\mathrm{ACC}} < \sigma_{\mathrm{POD}}$ (nine total) had scale height differences less than σ_{POD}. About 95% of the periapses with $\sigma_{\mathrm{ACC}} < 2\sigma_{\mathrm{POD}}$ (23 total) had scale height differences less then $2\sigma_{\mathrm{POD}}$. This percentage decreases to $\sim$68% for $\sigma_{\mathrm{ACC}} < 3\sigma_{\mathrm{POD}}$ (38 total), but these numbers indicate that the scale heights recovered by POD are representative of the

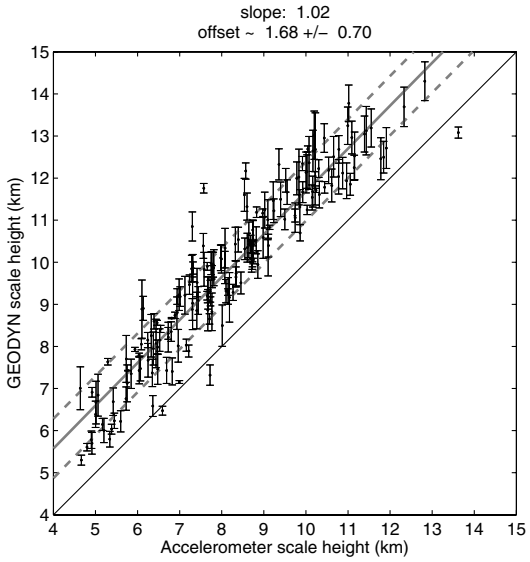

Fig. 8 Comparison of the POD-obtained scale heights versus the published accelerometer team values. The thick dark gray lines represent the best linear fit (dashed lines show 1-sigma uncertainties). The thin solid dark line represents the 1:1 line. The scale heights obtained from the tracking data are biased by $\approx +1.7$ km.

atmospheric density structure. When the atmosphere does not strictly follow an exponential profile, it still provides a picture of the effective drag environment experienced by the spacecraft during periapsis.

When no accelerometer data are available, these estimates would provide better constraints on scale heights than the values derived from the accelerometer experiments. Indeed using a simple exponential model, the POD scale heights will lead to the correct amount of orbital energy lost by friction, whereas lower scale heights (accelerometer) would underestimate it. The POD approach would be more appropriate to model the atmospheric structure from a navigation or orbit lifetime perspective. Indeed in the case of the Earth, early models based on satellite drag measurements (e.g., Jacchia models [19]) are still used operationally by various organizations (U.S. Air Force Space Command, NASA Marshall Space Flight Center) [20,21]. More recent models based on direct neutral density measurements (e.g., MSIS, mass spectrometer and incoherent scatter [22]) are more expensive computationally and do not lead to better accuracy [20]. In terms of orbit lifetime, the MSIS model tends to postpone the reentry date [23].

The density and scale heights near periapsis during the Mars Odyssey aerobraking can to first order be fitted linearly with latitude. The 1-σ fitting error for the scale height is about 13%, or 1.7 km, whereas for the density (in log scale) σ is close to 40%. Thus, if no accelerometer data are available, estimates of reasonable accuracy obtained from radio tracking data can be used to constrain the spacecraft drag environment.

V. Conclusions

We have demonstrated using observations from Mars Odyssey how precision orbit determination can be used to build on results from the accelerometer instrument during aerobraking to understand better the density structure of the Martian atmosphere. Using the spacecraft's X-band radio tracking data, we were able to tightly constrain the amount of energy lost by friction during each passage through periapsis. Although the density cannot be estimated directly because of the dependence of our results on the a priori atmospheric models used, the trajectory arcs prove useful to obtain improved estimates of the atmospheric scale height near periapsis. The effective atmospheric structure derived from POD consistently shows larger scale heights than those inferred from accelerometer data alone. This technique, which could be applied to other spacecraft with an accelerometer experiment (such as MGS and

MRO), can be useful for engineering and navigation purposes. Indeed the temporal resolution of our measurements (one per orbit) is very poor compared with the accelerometer (typically 1 per second), but the observations relate directly to the effective energy lost by the spacecraft drag passes. The radio science measurements constitute a data set that could be used to estimate the effects of atmospheric drag on the orbit when no accelerometer data are available, and yield accurate atmospheric density estimates when the atmosphere is well approximated by an exponential density structure.

Acknowledgments

This work was funded by the Mars Critical Data Products Program. We thank two anonymous reviewers for helping improve the manuscript.

References

[1] Keating, G. M., Bougher, S. W., Zurek, R. W., Tolson, R. H., Cancro, G. J., Noll, S. N., Parker, J. S., Schellenberg, T. J., Shane, R. W., Wilkerson, B. L., Murphy, J. R., Hollingsworth, J. L., Haberle, R. M., Joshi, M., Pearl, J. C., Conrath, B. J., Smith, M. D., Clancy, R. T., Blanchard, R. C., Wilmoth, R. G., Rault, D. F., Martin, T. Z., Lyons, D. T., Esposito, P. B., Johnston, M. D., Whetzel, C. W., Justus, C. G., and Babicke, J. M., "The Structure of the Upper Atmosphere of Mars: In Situ Accelerometer Measurements from Mars Global Surveyor," *Science*, Vol. 279, No. 5357, 1998, p. 1672.

[2] Withers, P. G., Bougher, S. W., and Keating, G. M., "The Effects of Topographically Controlled Thermal Tides in the Martian Upper Atmosphere as Seen by MGS Accelerometer," *Icarus*, Vol. 164, No. 1, 2003, pp. 14–32.

[3] Tolson, R. H., Keating, G. M., George, B. E., Escalera, P. E., Werner, M. R., Dwyer, A. M., and Hanna, J. L., "Application of Accelerometer Data to Mars Odyssey Aerobraking and Atmospheric Modeling," *Journal of Spacecraft and Rockets*, Vol. 42, No. 3, 2005, pp. 435–443.

[4] Withers, P. G., "Mars Global Surveyor and Mars Odyssey Accelerometer Observations of the Martian Upper Atmosphere During Aerobraking," *Geophysical Research Letters*, Vol. 33, 2006, p. L02201.

[5] Tracadas, P. W., Zuber, M. T., Smith, D. E., and Lemoine, F. G., "Density Structure of the Upper Thermosphere of Mars from Measurements of Air Drag on the Mars Global Surveyor Spacecraft," *Journal of Geophysical Research*, Vol. 106, No. E10, 2001, pp. 23,349–23,358.

[6] Bruinsma, S., and Lemoine, F. G., "A Preliminary Semiempirical Thermosphere Model of Mars: DTM-Mars," *Journal of Geophysical Research*, Vol. 107, No. E10, 2002, p. 5085.

[7] Forbes, J. M., Bruinsma, S., and Lemoine, F. G., "Solar Rotation Effects in the Thermospheres of Mars and Earth," *Science*, Vol. 312, No. 5778, 2006, pp. 1366–1368.

[8] Mazarico, E., Zuber, M. T., Lemoine, F. G., and Smith, D. E., "Martian Exospheric Density Using Mars Odyssey Radio Tracking Data," *Journal of Geophysical Research*, Vol. 112, No. E5, 2007, p. E05014.

[9] Lemoine, F. G., Bruinsma, S., Chinn, D. S., and Forbes, J. M., "Thermospheric Studies with Mars Global Surveyor," *Journal of Spacecraft and Rockets* (to be published).

[10] Keating, G. M., Murphy, J. R., Beebe, R. F., and Huber, L. F., ODY-M-ACCEL-5-ALTITUDE-V1.0, NASA Planetary Data System, 2004.

[11] Konopliv, A. S., Yoder, C. F., Standish, E. M., Yuan, D.-N., and Sjogren, W. L., "A Global Solution for the Mars Static and Seasonal Gravity, Mars Orientation, Phobos and Deimos Masses, and Mars Ephemeris," *Icarus*, Vol. 182, No. 1, 2006, pp. 23–50.

[12] King-Hele, D., *Satellite Orbits in an Atmosphere: Theory and Applications*, Blackie, Glasgow, 1987.

[13] Acton, C. H., "Ancillary Data Services of NASA's Navigation and Ancillary Information Facility," *Planetary and Space Science*, Vol. 44, No. 1, 1996, pp. 65–70.

[14] Pavlis, D. E., Poulose, S. G., and McCarthy, J. J., "GEODYN Operations Manuals," *Contractor Report*, SGT, Inc., Greenbelt, MD, 2006.

[15] Standish, D. E., Newhall, X. X., Williams, J. G., and Folkner, W. M., "JPL Planetary and Lunar Ephemerides, DE410," Jet Propulsion Laboratory, California Inst. of Technol., Tech. Rept. JPL IOM 312. N.03-007, 2003.

[16] Jacobson, R. A., "Ephemerides of the Martian Satellites," Jet Propulsion Laboratory, California Inst. of Technol., Tech. Rep. JPL IOM 312.1-95-142, 1995.

[17] Lemoine, F. G., Smith, D. E., Rowlands, D. D., Zuber, M. T., Neumann, G. A., Chin, D. S., and Pavlis, D. E., "An Improved Solution of the Gravity Field of Mars (GMM-2B) from Mars Global Surveyor," *Journal of Geophysical Research*, Vol. 106, No. E10, 2001, pp. 23,359–23,376.

[18] Stewart, A. I. F., "Revised Time Dependent Model of the Martian Atmosphere for Use in Orbit Lifetime and Sustenance Studies," Univ. of Colorado, Tech. Rept. JPL PO NQ-802429, 1987.

[19] Jacchia, L. G., "Static-Diffusion Models of the Upper Atmosphere with Empirical Temperature Profiles," Smithsonian Astrophysical Observatory Special Report No. 170, 1964.

[20] Marcos, F. A., "New Satellite Drag Modeling Capabilities," *Proceedings of the 44th AIAA Aerospace Sciences Meeting*, 2006.

[21] Marcos, F. A., Bowman, B. R., and Sheehan, R. E., "Accuracy of Earth's Thermospheric Neutral Density Models," *AIAA/American Astronomical Society Astrodynamics Specialist Conference*, 2006.

[22] Hedin, A. E., Reber, C. A., Newton, G. P., Spencer, N. W., Brinton, H. C., Mayr, H. G., and Potter, W. E., "A Global Thermospheric Model Based on Mass Spectrometer and Incoherent Scatter Data: MSIS 2 Composition," *Journal of Geophysical Research*, Vol. 82, June 1977, pp. 2148–2156.

[23] Pardini, C., and Anselmo, L., "On the Accuracy of Satellite Reentry Predictions," *Advances in Space Research*, Vol. 34, No. 5, 2004, pp. 1038–1043.

A. Ketsdever
Associate Editor